International Journal of Engineering Innovation & Research
Volume 2, Issue 5, ISSN: 2277 – 5668

Sputtered NbN Films on MS with Cr and EN Interlayer

Kulwant Singh
FRMS, Materials Group, BARC,
Trombay, Mumbai - 400085, India
Email: singhkw@barc.gov.in

N. Krishnamurthy
FRMS, Materials Group, BARC,
Trombay, Mumbai - 400085, India

A. K. Suri
Former Director, Materials Group,
BARC, Trombay, Mumbai - 400085, India

***Abstract* – Objective of the present study was to explore the benefits of NbN coating on MS with Cr and EN interlayer. NbN films were deposited by reactive DC magnetron sputtering on MS, SS and MS with Cr and EN interlayer in 2, 4 and 10 µm thicknesses. N_2/Ar flow ratio was varied 0-70%. Substrate biasing was varied from 0 to -150V. Effect of N_2 flow and substrate biasing was studied on the deposition rate, crystal structure, hardness and adhesion. Cr was deposited by electroplating and EN was deposited by electroless plating. The duplex coatings were studied for the improvement with respect to surface hardness by Knoop micro indentation and corrosion performance by potentiodynamic polarization technique 1N H_2SO_4 solution at room temperature.**

Surface hardness increased from 1084HK_{25} (for NbN coating on MS) to 1672, 1985 and 2167HK_{25} respectively when Cr was incorporated as interlayer in 2, 4 and 10 µm thicknesses. EN increased the hardness to a lesser extent to 1436, 1564 and 1612HK_{25} respectively with 2, 4 and 10µm interlayer thickness. Cr was more effective in providing the load support. For corrosion protection, NbN coating alone could not protect the MS substrate effectively. However, when incorporated with either Cr or EN interlayer, there was an enormous increase in corrosion resistance. I_{corr} decreased from 150.2µA/cm^2 (for NbN coating on MS) to 25.4, 12.3 and 2.5µA/cm^2 with 2, 4 and 10µm thick Cr interlayer respectively. EN as interlayer was more effective and decreased the I_{corr} to 2.3, 0.37 and 0.35µA/cm^2 with 2, 4 and 10 µm thick interlayer respectively.

***Keywords* – Magnetron-Sputtering, NbN, Chromium, EN.**

I. INTRODUCTION

Compound coatings are prepared by many techniques. Sputtering is one of them [1], [2]. Binary, ternary or multi component compound coatings, multilayers, duplex coatings, nano-crystalline coatings are increasingly being researched, because of their exotic properties such as high hardness, high wear resistance, low friction, high corrosion resistance etc. Niobium nitride (NbN) films in the initial years were investigated more because of their superconducting properties rather than their mechanical properties. The work on synthesis of NbN films, initially, was directed to increase their superconducting transition temperatures [3], [4]. However, NbN films are attractive in wear applications too because of their good thermal expansion match with widely used tool steels. Good mechanical properties coupled with chemical inertness, wear resistance, high melting point, temperature stability and high electrical conductivity make NbN films a suitable material for protective coating [5], field emission cathode [6] and diffusion barrier in microelectronic devices [7]. NbN thin films have been prepared by various deposition techniques including reactive magnetron sputtering [8], [9], ion beam assisted deposition [10], pulsed laser deposition [11] and cathodic arc deposition [12]. After the introduction of super lattice coatings, NbN was used as one layer component. Super lattice coatings such as TiN/NbN [13], TaN/NbN [14] and CrN/NbN [15] have been investigated for use as hard, wear resistant and corrosion protective coatings. Super lattice films possess super-hardness effects, which exhibit an anomalous increase in their hardness and wear resistance. NbN coatings with interlayer, however, have not been concerted upon. Hybrid coatings involving duplex technologies such as TiN coatings - deposited by sputtering with interlayer of chromium (Cr) and nickel (Ni) deposited by electroplating and electroless nickel (EN) deposited by electroless plating have been found to improve hardness, corrosion resistance and other properties when extended on to the mild steel (MS) substrates [16], [17], [18].

Objective of the present study was to explore the benefits of NbN hard nitride coating on MS substrate. However, deposition of hard nitride coatings on MS requires interlayer, because of two reasons. First, nitride coatings being too hard (hardness about 2000VHN) as compared to MS (hardness about 250VHN) require load support; second, hard nitride coatings deposited by Physical Vapour Deposition (PVD) techniques invariably have pin-hole porosity, which may not (corrosion) protect the underneath MS substrate effectively. Therefore, to take care of both these problems, provision of interlayer on MS with hard nitride coatings is a suitable option. In the present study, NbN coating were therefore studied with Cr and EN interlayer. NbN coatings were deposited by reactive magnetron sputtering. Cr was deposited by electroplating, whereas EN was deposited by electroless plating in various thicknesses. NbN coatings were deposited on stainless steel (SS) coupons and process parameters were optimized. NbN coatings were studied for crystal structure, thickness, hardness and adhesion with respect to N_2 flow rate and substrate biasing. NbN coatings were then deposited at optimized parameters on MS substrate as such and with Cr and EN interlayer in various thicknesses. Duplex coatings were studied for the improvement with respect to surface hardness by Knoop micro indentation and corrosion performance by potentiodynamic polarization technique. Open circuit potential (OCP) was also measured.

II. EXPERIMENTAL PROCEDURE

NbN films were deposited by reactive DC magnetron sputtering on SS, MS and Cr and EN plated MS coupons of 40mm×25mm×3mm size. A Niobium (99.98% purity)

metallic target 160mm diameter and 4mm thick was mechanically clamped to a planar sputter source mounted horizontally on the base of the chamber evacuated to a base pressure of 2×10^{-4} Pa. The distance between the target and the substrate was set at 60mm. The sputtering pressure was kept at 0.5Pa by admitting a stream of mixed gas of Argon (Ar) and nitrogen (N_2) into the chamber. Flow of Ar gas was fixed at 20sccm while N_2 flow was varied from 0-14sccm. Substrate biasing was kept constant at –50V for coatings deposited at different N_2/Ar flow ratios. The power to the target was supplied through a stabilized d. c. power supply of 0-1000V (6 Amperes maximum). Substrate biasing was varied from 0 to -150V in a step of 25V (keeping the N_2/Ar flow ratio constant at 20%) by means of a stabilized d. c. power supply of variable voltage (0-300V) and current (0-500mA). The samples were polished, cleaned thoroughly and degreased in alkaline solution prior to deposition. Proprietary mixtures were used for this purpose. The flow sheet used for cleaning of the samples before deposition is presented in the Fig.1. All the cleaning steps were performed ultrasonically for the specified duration. The MS samples were plated with Cr and EN as interlayer with NbN top coating. For plating, the samples were etched in 30% HCl after rinsing with distill water. It is necessary to ensure complete surface wetting, such that water film covers the sample surface before plating. The composition of bath used and operating parameters for electroplating of Cr and electroless plating of EN are listed in Tables 1 and 2 respectively. Cr and EN thickness was controlled to 2, 4 and 10 µm by varying the duration of plating. The rate of deposition was first determined on separate samples plated under similar conditions.

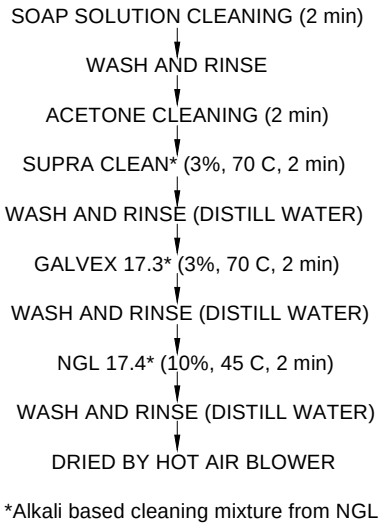

Fig.1. Cleaning cycle adopted

Table 1: Composition and parameters for Cr plating

Parameter	Value
Chromium trioxide	250 g/l
Sulphuric acid	2.5 g/l
Anode (material)	Antimonial lead
Temperature	55-60^{0}C
Cathode current Density	200 mA/cm^2

Coating thicknesses were found out using Calotest technique, where 52100 steel ball was rotated against coated samples using suspension of diamond particles. The phase structure of the films was investigated by X-ray diffraction (XRD) with CuKα radiation. Surface hardness was measured by a microhardness tester (Future Tech FM-7 model) using Knoop indenter at loads of 100, 50 and 25gf. Five readings were performed for each of the coated sample and the average values are reported.

Table 2: Composition and parameters for EN plating

Parameter	Value
Nickel chloride	35 g/l
Sodium citrate	20 g/l
Sodium hypophosphite	20 g/l
Stabilizer	1-2 ppm
Agitation of bath	Continuous
Temperature	~ 90^{0}C
pH	4.4 - 4.6

NbN coatings on MS and SS were evaluated for their adhesion performance by scratch tester. Effect of loading rate was studied at 10, 20, 30, 50, and 80N/min. Since the variation in loading rate had little impact, further scratch tests were carried out at 30N/min loading rate. The scratch length was 3mm. The scratch indenter used was a 200µm tip radius Rockwell type diamond indenter. Friction force and depth of indentation for all the scratched samples were recorded online. The scratch tracks were seen in the optical microscopy immediately after the tests to visualize the scratch pattern and pictures were taken at different loads. The starting load in each test was 1N while maximum load was varied from 10N to 60N. Tests were performed in a linearly progressive mode from 1N start load to a predefined maximum load.

Corrosion study of the samples was carried out using the standard potentiodynamic measurement technique with a computer controlled Santronic Electrochemical Analyzer. Tests were carried out using a three-electrode cell. One side coated samples were soldered (with indium) on the other side to a copper wire coated with enamel. The samples were masked by Shailmask 800 lacquer (proprietary) to get the 1cm^2 surface area exposed. All potentials were measured with respect to a saturated calomel electrode (SCE). The auxiliary or counter electrode was platinum. The anodic and cathodic electrochemical polarization curves of all the samples were obtained in nitrogen de-aerated 1N H_2SO_4 electrolyte at room temperature. Open circuit potentials (OCP) were measured in deaerated 1N H_2SO_4 solution for 2h. Before potentiodynamic measurements, the samples were allowed to reach equilibrium potential (E_{ocp}). This potential was reached after 30-40min and the electrochemical measurements were started when the potential did not change by more than 1mV/min. The solution was replaced after each sweep run. Polarization resistance was determined in the ±15mV domain of E_{ocp} potential using the linear polarization method at a scan rate of 0.1mV/sec. Potentiodynamic studies were carried out with a potential sweep range of –1.000V to +1.000V with a scan rate of

0.5mV/sec. The plot of E measured against SCE v/s log I was plotted. The corrosion potential (E_{corr}) was determined from the intersection of Tafel slopes and corrosion current density (I_{corr}) was calculated using the anodic and cathodic Tafel slopes (β_a and β_c) and polarization resistance (R_p).

III. Results and Discussion

A. Thickness

Thickness of the coatings was calculated by weight gain method taking the bulk density value from the literature. Actual coating thicknesses were found out by the Calotest technique using micro abrasion by diamond particles. A variation of 5-15% was found between the calculated and actual values due to the density of the coatings being lower than the bulk value. In the deposition using biasing there is a continuous ion bombardment at the substrate, causing the reduced effective deposition rate, which in turn reduces the coating thickness and therefore more time was required to get the same coating thickness. Coating thickness of 1.8µm ±10% was obtained.

B. Deposition Rate

(i) Effect of Nitrogen Flow

Deposition rates of Nb-N coatings have been plotted in Fig. 2 as a function of N_2/Ar flow ratio. The coatings were deposited without biasing and at a constant substrate bias voltage of –50V. Deposition rate decreased from 20nm/min to 8.8nm/min (without biasing) and from 16nm/min to 6.6nm/min (with biasing at -50V) with the increase in N_2/Ar flow ratio from 0-70%. Deposition rate reduced almost linearly in both the cases with every increase in N_2 flow. The decrease in deposition rate, with every increase in nitrogen flow, was due to the increased nitridation of the target; well known as the poisoning of the target surface. Further, it was seen that the reduction in deposition rate followed three different linear paths in both the cases – with biasing or without biasing. The three linear decreases in deposition rates correspond to transition of phases from Nb to Nb_2N, Nb_2N to cubic NbN and cubic NbN to *h* NbN phase, as revealed by XRD.

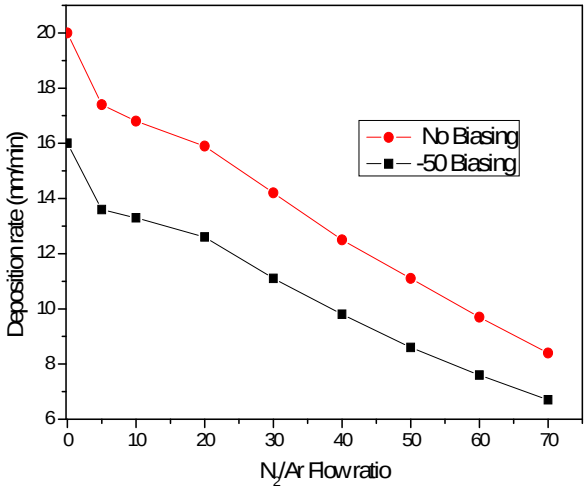

Fig.2. Deposition rate of Nb-N coating Vs N_2 flow

(ii) Effect of Substrate Biasing

Biasing causes continuous ion bombardment at the substrate, which imparts energy and thus not only improves adhesion, but also coating density. However, deposition rate is reduced. Fig. 3 shows the deposition rate plotted against the substrate bias voltage keeping the N_2 flow constant (F_{N2}/F_{Ar}=20%). Deposition rate decreased from 15.9nm/min to 6nm/min when the bias voltage (negative) was increased from 0 to 150V. The decrease in deposition rate with the increase in substrate biasing is due to the ion bombardment effect at the substrate. With every increase in substrate biasing (negative voltage) increased re-sputtering at the substrate with higher energy ions takes place. This causes removal of entrapped gas atoms, densification of the grain boundaries and re-sputtering of depositing particles, resulting in fall of deposition rates.

C. Hardness

(i) Effect of Nitrogen Flow

Knoop microhardness values for Nb-N coated samples on SS, taken at a load of 25gf, have been plotted as a function of increasing N_2 flow in figure 4 (substrate biasing was kept constant at –50V). Surface hardness increased rapidly with the increase in N_2 flow. Hardness reached a maximum of 2040HK_{25} at a N_2/Ar flow ratio of 20% and then started decreasing slowly with the further increase in N_2 flow. The decrease in hardness was accompanied with the observed changes in the crystalline structure of coatings as revealed by XRD. Grain size also influences the hardness of the materials. Hardness changes as per the Hall-Petch relationship. Grain size has been found to increase with the increase in the partial pressure of nitrogen [19], [20]. The decrease in hardness at higher partial pressures of nitrogen could also be attributed partly due to the increase in grain sizes.

Since, the maximum hardness obtained was at 20% N_2 flow, NbN on MS with Cr and EN interlayer was deposited at 20% of N_2 flow.

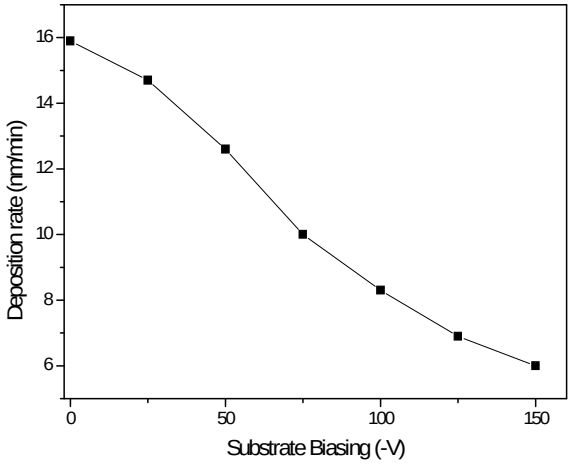

Fig.3. Deposition rate of Nb-N Vs substrate biasing

(ii) Effect of Substrate Biasing

Figure 5 shows the surface hardness plotted against the substrate bias voltage keeping the N_2/Ar flow ratio constant (at 20%). Hardness increases continuously with

the increase in substrate bias voltage. Hardness increased from 1692HK_{25} for coatings deposited without biasing to 2346HK_{25} for coatings deposited at -150V substrate biasing. Kim et al [21] observed the increase in hardness similarly with the increase in substrate bias up to -200V. The hardness enhancement by energetic ion bombardment is due to a complex, synergistic effect involving a decrease of crystallite size, densification of the grain boundaries, formation of radiation damage and other point defects, and built-in biaxial compressive stress [22].

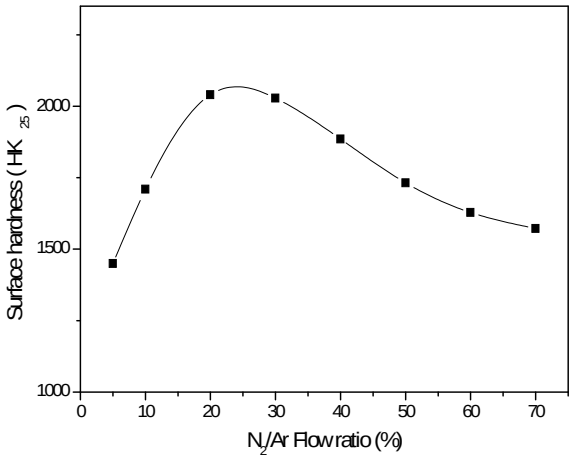

Fig. 4: Surface hardness of Nb-N Vs N_2 flow

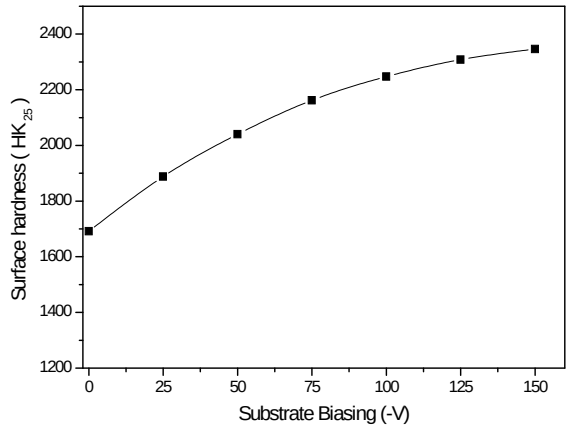

Fig.5. Surface hardness Vs substrate biasing

(iii) Duplex Coatings on MS

Surface hardness of MS substrate; Cr, EN, NbN coatings and NbN with Cr and EN interlayer on MS are given in Table 3. Cr plating, being hard showed the hardness of about 800-900HK. EN plating showed the hardness in the range of 500-600HK. Increase in hardness, in general, is evident with decrease in load and increase in the thickness of the deposit. Substrate effect is pronounced in the case of NbN on MS. Hardness of NbN coating increased from 487 to 1084HK with the decrease in applied load from 100 to 25gf. With the incorporation of Cr and EN interlayer, the hardness of NbN/MS increased due to the load support provided by the interlayer. Hardness also increased with the increase in thickness of the interlayer. Hardness was found to be 2167HK with 10µm Cr interlayer and 1612HK with 10µm EN interlayer at 25gf. Cr was more effective in providing the load support.

D. X-ray Diffraction

X-ray diffraction patterns of Nb-N films deposited on SS at various N_2/Ar flow ratios are shown in Fig. 6. Coatings deposited at 5% N_2 flow show hexagonal β Nb_2N as the major phase with (101) preferred orientation. With the increase in N_2 flow to 10%, major phase becomes cubic δNbN with preferred orientation of (111). At 30% N_2 flow hexagonal δ'NbN phase appears, though the major phase is still cubic δNbN but now with preferred orientation of (200). With the further increase in N_2 flow hexagonal δ'NbN phase increased and became major phase at 70% N_2 flow. In all the coatings substrate peaks were identified as the major peaks.

Table 3: Surface hardness for coatings on MS

Coating (thickness µm)	100gf	50gf	25gf
Substrate	182	186	198
Cr (2)	222	302	468
Cr (4)	434	492	672
Cr (10)	806	907	938
EN (2)	326	381	439
EN (4)	447	489	586
EN (10)	582	592	612
NbN	487	674	1084
Cr (2) + NbN	987	1180	1672
Cr (4) + NbN	1163	1436	1985
Cr (10) + NbN	1286	1616	2167
EN (2) + NbN	712	905	1436
EN (4) + NbN	892	1078	1564
EN (10) + NbN	1183	1246	1612

MS samples showed the peak of Fe(110) in the 2θ range performed. Cr coated samples showed the broadening of this peak, which also corresponds to Cr(110) peak, as the two are having similar structure and almost same lattice parameter. Fig. 7 shows the X-ray diffraction patterns of MS and NbN/MS. NbN coating showed the cubic δNbN phase with (111) peak stronger than (200) and (220) peaks.

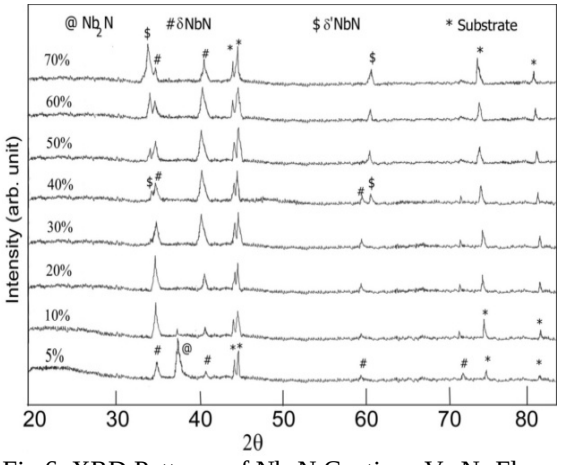

Fig.6. XRD Patterns of Nb-N Coatings Vs N_2 Flow

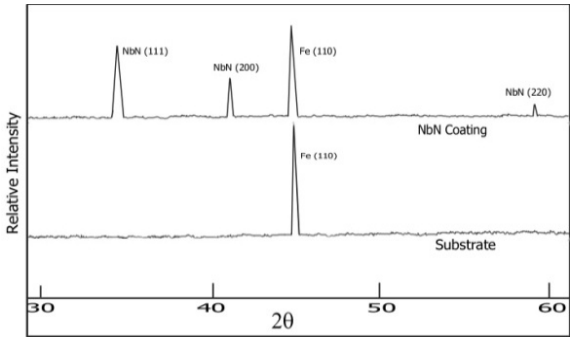

Fig.7. X-ray diffraction patterns for MS and NbN/MS

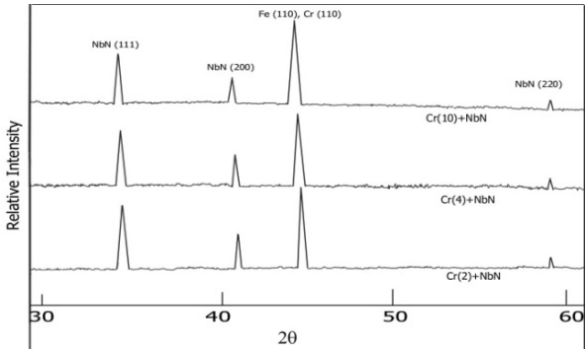

Fig.8. X-ray diffraction patterns for NbN/Cr/MS

Fig.8 shows the X-ray diffraction patterns of NbN coating with various thicknesses of Cr interlayer. With the increase in thickness of interlayer a slight shift in the combined peak of Fe(110) and Cr(110) was observed towards lower angle which implies an increase in the lattice parameter. This is in line with the values of lattice parameter of Fe (2.8664A^o) and Cr (2.8839A^o). At 10µm thick Cr interlayer, Cr(110) peak was found to be stronger than NbN peaks. Fig. 9 shows the X-ray diffraction pattern of EN/MS and NbN/MS with EN interlayer in various thicknesses. EN structure was amorphous having a diversion at Fe(110). Fe(110) peak was found to be shortening and getting broadened with the increase in thickness of EN. When NbN top-coat was given by sputtering on EN plated MS, several peaks of Ni_3P and Ni were evident. This clearly demonstrated the transformation of EN amorphous structure to crystalline during sputtering.

E. Scratch Adhesion Test

Friction force and depth of indentation for all the scratch tests were recorded online along with the indenter movement to confirm the critical loads for cracks, chipping, delamination, coating failure or other such observations. Tests performed at different loading rates gave almost similar results and variation in loading rate had little impact on the scratching behaviour. Several types of observations were revealed as the scratch progressed in a linearly increasing load mode, such as - top layers removal, pile-up on the sides, visibility of small cracks to long wide cracks within the coatings, pores, chipping, delamination of the coating etc. Fig. 10 shows the scratch pattern for NbN/MS at a load of (a) 7N showing cracks, pores and top layer removal and at (b) 12N load revealing cracks, chipping and partial delamination. Fig. 11 exhibits the scratch pattern for NbN/SS at 12N and 28N showing the segregation, cracks, pores, chipping, and pile-up increasing with the load.

(i) Critical Loads

Two critical loads Lc_1 and Lc_2 have been defined for the failure of the coatings. Lc_1, the first critical load, corresponds to initial cohesive failure of the coating such as appearance of first cracks or pores within the coating. Lc_2, the second critical load, corresponds to first adhesive failure of the coating such as chipping, partial delamination, pores or some such phenomena, where substrate beneath coating gets exposed. Lc_1 and Lc_2 values for NbN coating on MS samples were observed to be between 6-8N and 9-12N loads respectively. For coatings on SS substrates Lc_1 varied between 8-15N and Lc_2 varied between 12-25N for coatings deposited at various N_2 flow.

(ii) Coefficient of Friction

Coefficient of friction (µ) as observed in the scratch test varied with the scratch load. For coatings deposited on SS samples, it varied within a narrow range of 0.22-0.25 at 30N load irrespective of coatings deposited at different flow ratios of N_2. At 40N load, the value increased to 0.30 and at 60N load, the value was 0.40. For MS samples, the µ was 0.28 at 30N load, 0.35 at 40N load and 0.45 at 60N load. Table 4 lists the µ value at different loads for the two types of substrates.

Table 4: µ at different loads for NbN on MS and SS

Load(N)	MS	SS
20	0.23	0.20
30	0.28	0.25
40	0.35	0.30
60	0.45	0.40

(iii) Effect of Loading Rate

The effect of loading rate on Lc_1 and Lc_2 had little impact. The Lc_1 value shifted from 7N at 10N/min to7.5N at 30N/min and further to 8.2N at 50N/min. Similarly Lc_2 value shifted from 8.2N to 9N and further to 9.5N with similar increase in applied loading rate. For SS samples, the Lc_1 changed from 15 to 17N and Lc_2 changed from 22N to 24N, when the applied loading rate was increased successively from 20 to 80N/min.

(iv) Depth of Penetration

Depth of penetration increased with the increase in applied load. At 30N load, on an average, MS coated samples had 20-30µm depth of penetration while SS coated samples had 12-25µm depth of penetration. Depth of penetration includes elastic as well as plastic deformation during loading. Besides, there could be error factor due to slope of the samples (thickness variation in sample).

(v) Effect of Biasing

Increase in biasing voltage from 0 to –75V (in a step of 25V), keeping other factors constant during deposition of Nb-N coating on SS substrate, led to increase in Lc_1 and Lc_2. However at -100V, Lc_1 and Lc_2 both dropped drastically indicating the brittle nature of the coating. The values are shown in Table 5.

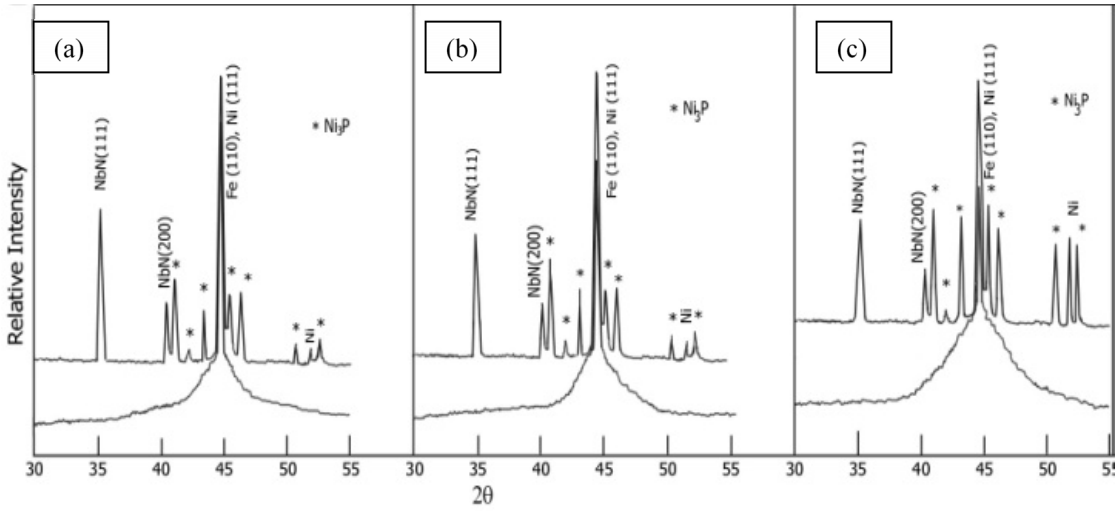

Fig.9. X-ray diffraction patterns for NbN/EN/MS with EN thickness (a) 2µm, (b) 4µm and (c) 10µm

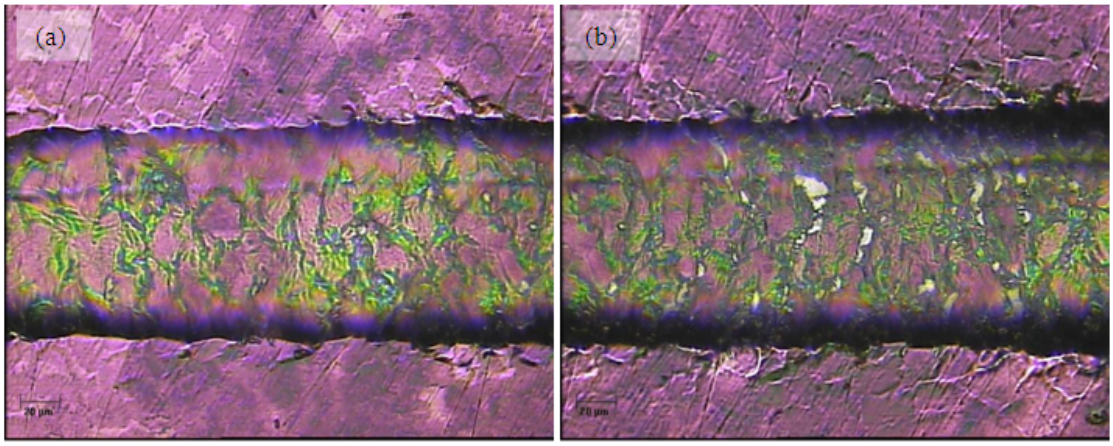

Fig.10. Scratch test for NbN/MS at (a) 7N and (b) 12N load

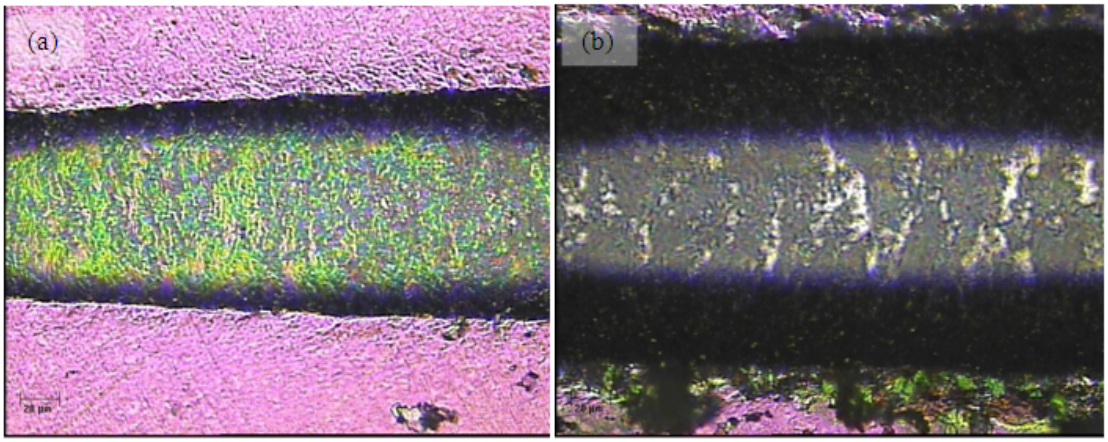

Fig.11. Scratch test for NbN/SS at (a) 12N and (b) 28N load

Table 5: Effect of biasing on critical loads for Nb-N/SS

Biasing (-V)	Lc_1	Lc_2
0	6.5	10.5
25	10.5	20
50	12.0	24
75	15.6	26
100	7.0	11

Table 6: Effect of N_2 flow on critical loads for Nb-N/SS

N_2/Ar Flow %	Lc_1	Lc_2
10	11	18
20	12	24
30	11	25
40	10	20
50	8	20
60	8	18
70	7	14

(vi)Effect of N_2 Flow

Nb-N/SS deposited at N_2/Ar flow ratios from 10% to 70%, (at constant bias of -50V), were tested by scratch tester. Results with respect to critical loads are shown in Table 6. Coatings deposited at 20 and 30% of N_2/Ar flow ratios showed better adhesion with higher critical loads.

F. Corrosion Resistance

It is difficult to deposit the hard coatings by PVD techniques without any porosity. Thus, when a PVD coated sample is exposed to the corrosive environment, the electrochemical behavior of the coated sample is the combined behavior of the coating and the substrate. The polarization curve of such a specimen may be considered as a combination of the two curves - one representing the base material, and the other the coating.

(i) Open Circuit Potential

Fig. 12 shows the changes in OCP with immersion time for NbN/MS with and without Cr interlayer. For NbN/MS, potential decreased from initial value of -252 to -478mV in 30min and to -498mV in 40min after which it remained nearly constant indicating the establishment of equilibrium between the metal and the solution. The equilibrium value was quite similar to MS substrate without coating, thus indicating the presence of pores in the coating, resulting in corrosion taking place beneath NbN coating. For NbN/Cr/MS, OCP's shifted to -34, -62 and -108mV in the beginning for 10, 4 and 2µm Cr interlayer respectively from -252mV for NbN coating without interlayer. The values decreased to -348, -401 and -447mV for 10, 4 and 2µm thick Cr interlayer after 30min. The values further decreased slightly after 40min and remained constant thereafter. Figure 13 shows the changes in OCP with immersion time for NbN/MS with EN interlayer. The OCP's in the beginning shifted to -82, -98 and -112mV for 10, 4 and 2µm thick EN interlayer respectively. The values decreased to -324, -346 and -352mV for 10, 4 and 2µm thick EN interlayer coatings in 40min. The values remained constant thereafter.

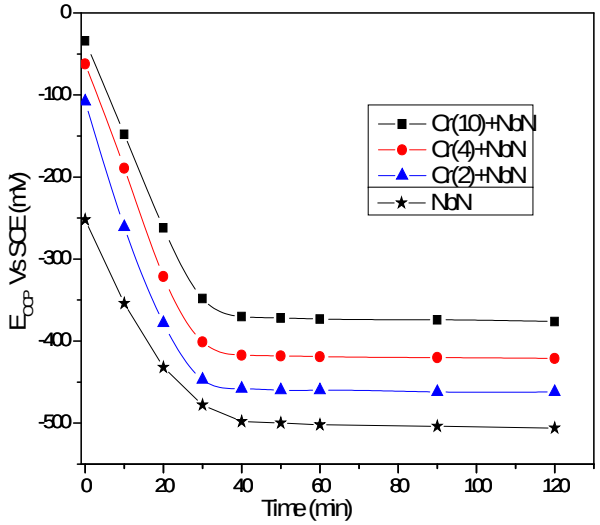

Fig.12. E_{OCP} Vs time for NbN/MS and NbN/Cr/MS

(ii) Potentiodynamic tests

E_{corr} and I_{corr}, were determined from their polarization curves using the Tafel slopes β_a and β_c and polarization resistance (R_p). A high E_{corr} and a low I_{corr} values are indicative of good corrosion resistance.

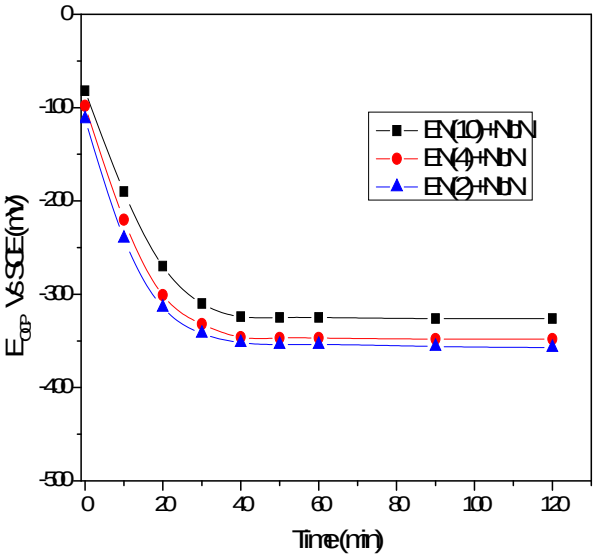

Fig.13: E_{OCP} Vs time for NbN/EN/MS

Table 7: E_{corr} and I_{corr} values for coatings on MS

Coating (thickness µm)	E_{corr} (mV)	I_{corr} (µA/cm^2)
MS Substrate	-496.4	1440.3
NbN	-412.1	150.2
Cr (2)	-476.6	704.9
Cr (4)	-463.2	643.7
Cr (10)	-442.3	527.5
EN (2)	-339.3	8.6
EN (4)	-330.4	0.24
EN (10)	-214.3	0.21
Cr (2) + NbN	-440.7	25.4
Cr (4) + NbN	-428.4	12.3
Cr (10) + NbN	-398.6	2.5
EN (2) + NbN	-320.3	2.3
EN (4) + NbN	-294.6	0.37
EN (10) + NbN	-220.6	0.35

Table 7 lists the E_{corr} and I_{corr} values for MS substrate; NbN, Cr and EN films on MS and NbN with Cr and EN interlayer in different thicknesses on MS. Plain MS substrate had E_{corr} value of -496.4mV and I_{corr} value of 1440µA/cm^2. Coating the MS sample with NbN improved the corrosion resistance by decreasing the I_{corr} to 150µA/cm^2 and increasing the E_{corr} (less negative) to -412mV. However, the improvement was constrained due to the presence of pin-hole porosity inherent in PVD coatings. Due to the presence of pin-hole defects in the NbN coatings, in fact rapid pitting corrosion of MS substrate took place at these defects; even leading to partial debonding of the coating. The potentiodynamic curves for NbN coatings, therefore, mimic the behavior of MS substrate (Fig. 14).

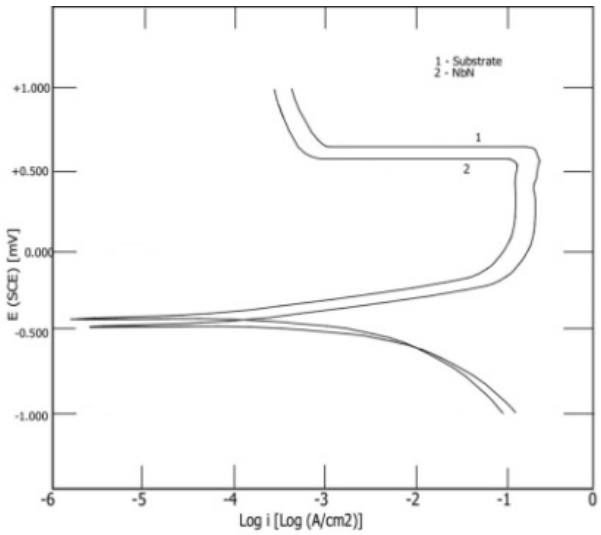

Fig.14. Potentiodnamic curves for MS and NbN/MS

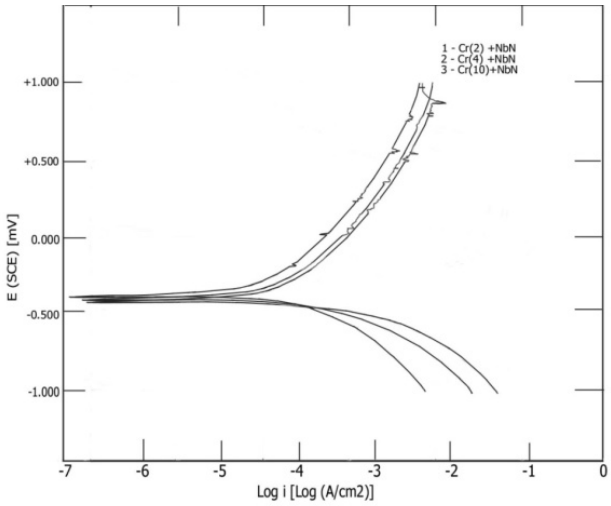

Fig.15. Potentiodynamic curves for NbN/Cr/MS

Though Cr and EN both as interlayer improved the corrosion resistance of NbN coated MS substrate remarkably; EN was found to be superior. Increase in thickness of the interlayer also improved the corrosion resistance. For 10µm thick Cr interlayer E_{corr} and I_{corr} were -398.6mV and 2.5µA/cm^2 respectively; for 10µm thick EN interlayer E_{corr} and I_{corr} were -220.6mV and 0.35µA/cm^2 respectively. With the duplex coating, the adherence also improved, because none of the coatings was found to delaminate for the full potential sweep of -1000mV to +1000mV during the potentiodynamic corrosion tests performed for all the interlayer thicknesses. Fig. 15 depicts the potentiodynamic curves for NbN coating with Cr interlayer; whereas Fig. 16 depicts the potentiodynamic curves for NbN coating with EN interlayer. Potentiodynamic curves for the duplex coatings showed a remarkable improvement in the corrosion resistance for MS substrate with respect to NbN coating alone. However, for corrosion protection, EN was found to be more effective than Cr.

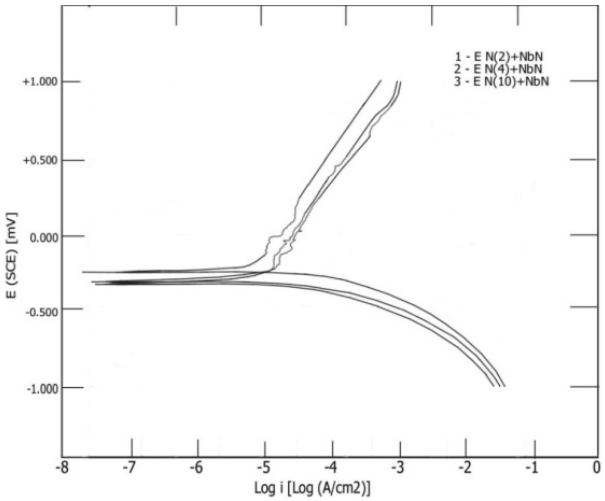

Fig.16. Potentiodynamic curves for NbN/EN/MS

REFERENCES

[1] Jianliang Lin, John J. Moore, William D. Sproul, Brajendra Mishra, Zhili Wu, Jun Wang, *Surf. Coat. Technol*., 204 (2010) p. 2230

[2] A. Ravi Shankar, B. Prabhakara Reddy, Vipin Chawla, M. Jeya Preyanga, Ramesh Chandra, U. Kamachi Mudali, *Surf. Coat. Technol*., 204 (2010) p.3214

[3] D.F. Dawson-Elli, C.A. Fung, J.E. Nordman, *IEEE Trans. Magnetics*, 27 (1991) p.1592

[4] W.N. Maung, D.P. Butler, C.L. Huang, *J. Vac. Sci. Technol. A* 11 (1993) p.615

[5] Benkahoul M, Martinez E, Karimi A, Sanjin´es R and L´evy F, *Surf. Coat. Technol*., 180 (2004) p.178

[6] Gotoh Y, Nagao M, Ura T, Tsuji H and Ishikawa *J. Nucl. Instrum. Methods Phys. Res. B* 148 (1999) p.925

[7] Al´en P, Ritala M, Arstila K, Keinonen J and Leskel¨a M, *Thin Solid Films*, 491 (2005) p.235

[8] J.J. Olaya, S.E. Rodil, S. Muhl, *Thin Solid Films*, 516 (2008) p. 8319

[9] M. Fenker, M. Balzer, H. Kappl, *Thin Solid Films*, 515 (2006) p.27

[10] Klingenberg M L and Demaree J D, *Surf. Coat. Technol*., 146 (2001) p.243

[11] G. Cappucio, U. Gambardella, A. Morone, S. Orlando, G.P. Parisi, *Appl. Surf. Sci*. 109 (1997) p.399

[12] N. Cansever, M. Danışman, K. Kazmanlı, *Surf. Coat. Technol*., 202 (2008) p.5919

[13] Harish C. Barshilia, K.S. Rajam, D.V. Sridhara Rao, *Surf. Coat. Technol*., 200 (2006) p.4586

[14] X. Junhua, G. Mingyuan, L. Geyang, *J. Mater. Sci*. 35 (14) (2000) p.3535

[15] D.B. Lewis, S.J. Creasey, C. Wüstefeld, A.P. Ehiasarian, P.Eh. Hovsepian, *Thin Solid Films*, 503 (2006) p.143

[16] K. Singh, A. K. Grover, M. K. Totalani, A. K. Suri, *Trans. IMF*, 78(1) (2000) p.23

[17] K. Singh, A. K. Grover, M. K. Totalani, A. K. Suri, *Trans. IMF*, 77(5) (1999) 196-199

[18] V.K. William Grips, V. Ezhil Selvi, Harish C. Barshilia, K.S. Rajam, Electrochimica Acta, 51(17) (2006) p.3461

[19] Li-Jian Meng and M.P. dos Santos, *Surf. Coat. Technol*. 90 (1997) p.64

[20] R. Wuhrer, W.Y. Yeung, *Materials Forum*, 29 (2005) p.103

[21] S.K. Kim, B.C. Cha and J.S. Yoo, *Surf. Coat. Technol*., 177–178 (2004) p.434

[22] S. Veprek, M.G.J. Veprek-Heijman, P. Karvankova, J. Prochazka, *Thin Solid Films*, 476 (2005) p.1

AUTHOR'S PROFILE

Kulwant Singh

is working as a scientist G in FRMS, Materials Group, BARC, Trombay, Mumbai. He did B. Tech in Metallurgical Engg. from IIT, Roorkee and has submitted the thesis for PhD at Mumbai University. He is working on the development of hard, wear and corrosion resistant nitride coatings by Magnetron Sputtering and their characterization by various techniques. He has also worked on the extraction and Refining of Nb and V metals from their ferroalloys. His areas of expertise include surface engineering, characterization and performance evaluation of coatings, process metallurgy, and failure analysis.

Dr. N. Krishnamurthy

is an outstanding scientist at Bhabha Atomic Research Centre, Trombay, Mumbai, India and is heading the Fusion Reactor Materials Section at the centre. He is also an Honorary Professor of Homi Bhabha National Institute, Mumbai and has been teaching 'Thermodynamics and Extractive Metallurgy' to Metallurgy Trainee Scientists. He is B.Sc. (Chemistry), M.Sc. (Chemistry), and PhD (Chemistry). He is working on new and improved processes for reactive and refractory metals, thorium and rare earths. His areas of expertise include extractive metallurgy (reduction and refining), thermodynamics, and phase diagrams. His fields of interests include Application of thermodynamics to process metallurgy of refractory and reactive metals, computation and determination of phase diagrams, thermodynamic measurements and calculations.

Dr. A. K. Suri

Former Director, Materials Group, BARC has wide variety of experience in various fields related to Metallurgy and Materials Science. He did BE (Metallurgy), MS (Metall. & Mater Sci.) and Ph.D. (Metallurgy). He Set up a Tin Demonstration Plant for MP State Mining Corporation at Raipur in 1985, was involved in setting up a Demonstration Plant for Department of Ocean Development at Hindustan Zinc Ltd., Udaipur, for processing of ocean nodules in 2002, Setting up of specific facilities for processing of heavy metals, and Setting up of Technology Demonstration Plant at UCIL, Jaduguda in 2005. He has been instrumental in the following products development - Boron carbide, Metal and alloy borides, Tin metal and powder, and Organic extractants.